

# Sampling Strategy Selection for EMC Simulation Surrogate Model in Uncertainty Analysis and Electromagnetic Optimization Design

Shenghang Huo, Jinjun Bai\*, Shaoran Gao, and Yule Liu

*College of Marine Electrical Engineering, Dalian Maritime University, Dalian 116026, China*

**ABSTRACT:** Surrogate models have been gradually promoted in electromagnetic compatibility (EMC) simulation in recent years, and two typical application scenarios are uncertainty analysis and electromagnetic optimization design. The surrogate model can simulate the forward EMC simulation process as accurately as possible with relatively few sampling points. The choice and number of sampling points will directly determine the accuracy of the surrogate model. The purpose investigated by uncertainty analysis and electromagnetic optimization design is different. How to choose appropriate sampling strategies is worth discussing, but there are very few studies in the field at this stage. This paper applies a cascaded cable crosstalk example to explore the accuracy of the surrogate model under different sampling strategies, which provides a theoretical level of suggestion for the application of the surrogate model in EMC simulation. The study enables the surrogate model to be better suited for two application scenarios: uncertainty analysis and electromagnetic optimization design.

## 1. INTRODUCTION

Surrogate models are black box-like models constructed by a small number of sampling points. Typical surrogate models include Least Squares Support Vector Regression (LSSVR) [1], Kriging [2], and Radial Basis Function (RBF) [3]. Currently, the surrogate model has been successfully applied in EMC simulation. Its application in two scenarios, i.e., uncertainty analysis and electromagnetic optimization design, is among the current research trends. In uncertainty analysis, the common methods include Stochastic Galerkin Method [4] and Stochastic Collocation Method [5] based on chaos polynomials. In electromagnetic optimization design, common methods are particle swarm optimization algorithms and genetic algorithms among other methods. The surrogate models have been used in both fields due to their efficiency and accuracy. Li et al. apply the Kriging model to optimize the design of photonic bandgap structures [6]. An approximate functional relationship between the photonic crystal bandgap and the design parameters is established using the Kriging surrogate model, which replaces the expensive reanalysis method in the electromagnetic field simulation of three-dimensional periodic structures. In [7], an improved Kriging model is proposed which performs EMC uncertainty simulation efficiently and accurately.

These surrogate models are constructed in essentially the same way. That is, sampling points are obtained by certain sampling methods, and deterministic EMC simulation is performed on the sampling points. The {sampling point, EMC simulation result} pairs are used as the training set to train the surrogate model. During the selection of sampling points, different

sampling strategies can result in varying sampling points even when using the same sampling method, thereby affecting the accuracy of the constructed surrogate model.

Surrogate models employ numerous sampling strategies in the field of mathematical theory, but relatively few have been examined in existing EMC simulation studies. Most of the EMC simulations based on surrogate models applied are based on the Latin hypercube sampling method with the static sampling strategy. In the field of EMC simulation, uncertainty analysis and electromagnetic optimization design are two current research trends, and their goals are different. Both uncertainty analysis and electromagnetic optimization design need the surrogate model to be able to predict the forward electromagnetic simulation process. While electromagnetic optimization design is more concerned with whether the optimal point can be searched and the accuracy of the optimal point neighborhood, uncertainty analysis is more concerned with the overall accuracy. Therefore, it is obviously unreasonable to use the same sampling strategy in these two application scenarios. The focus of this research is to explore how to select suitable sampling strategies based on different needs when applying the EMC simulation surrogate model to uncertainty analysis and electromagnetic optimization design. This ensures the accuracy of the surrogate model, enabling efficient and accurate solutions to these problems in EMC simulation.

The structure of this paper is as follows. Section 2 describes the application of the surrogate model to uncertainty analysis and electromagnetic optimization design. Section 3 describes the sequential addition strategy and static sampling strategy. A cascaded cable crosstalk example is presented in Section 4 to

\* Corresponding author: Jinjun Bai (baijinjun@dlmu.edu.cn).

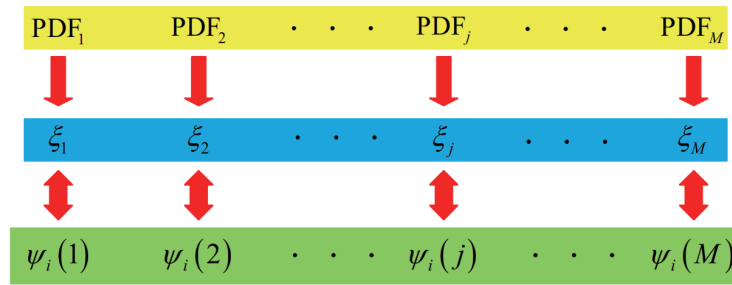


**FIGURE 1.** The relationship between random variables and exhaustive sampling points.

better enable the comparison of the performance of different sampling strategies in uncertainty analysis and electromagnetic optimization design. In Section 5, two sampling strategies are applied to uncertainty analysis and electromagnetic optimization design based on the Kriging model in order to investigate the applicability of different sampling strategies in uncertainty analysis and electromagnetic optimization design. Section 6 provides prospects for future research work. Section 7 summarizes this paper.

## 2. UNCERTAINTY ANALYSIS AND ELECTROMAGNETIC OPTIMIZATION DESIGN BASED ON SURROGATE MODEL

Uncertainty analysis and electromagnetic optimization design are both current research trends in the field of EMC simulation. Uncertainty analysis and electromagnetic optimization design based on surrogate models have attracted much attention due to their efficiency and accuracy. Regardless of the field to which it is being applied, the surrogate model needs to be trained with a set of training sets ( $S_{\text{EMC}}, Y_{\text{EMC}}$ ). The sample space  $S_{\text{EMC}} = [x_1, x_2, \dots, x_{n1}]$  in the training set ( $S_{\text{EMC}}, Y_{\text{EMC}}$ ) is  $n1$  sampling points obtained based on a certain sampling strategy. Each sampling point  $x_i$  is  $M$ -dimensional vector data as follows.

$$x_i = \{x_i(1), x_i(2), \dots, x_i(M)\} \quad (1)$$

where  $x_i(j)$  are all deterministic constant values. The deterministic EMC simulation is performed on each sample point  $x_i$ , and the simulation results obtained are as follows.

$$y_i = \text{EMC}[x_i] \quad (2)$$

where  $\text{EMC}[\ ]$  represents the deterministic EMC simulation process.  $y_i$  is the result of a single EMC simulation, which usually has a dimension other than  $M$  and needs to be specified according to the EMC simulation solver.  $Y_{\text{EMC}} = [y_1, y_2, \dots, y_{n1}]$  is the set of deterministic EMC simulation results.

In this paper, the Kriging model, which is currently popular in the field of EMC simulation, is selected for uncertainty analysis and electromagnetic optimization design based on different sampling strategies. The Kriging model is a classical surrogate model, which is representative, and its details are described in [6]. The Kriging model constructed by applying the training set ( $S_{\text{EMC}}, Y_{\text{EMC}}$ ) is denoted by  $M_{\text{Kriging}}[\ ]$ .

### 2.1. Uncertainty Analysis

In practical engineering, the sources of uncertainty can be categorized into stochastic uncertainty factors and cognitive uncertainty factors. Stochastic uncertainty factors mainly refer to cognitively clear but unavoidable randomness, such as random displacement caused by motion or vibration, randomness of the geometric structure of cable bundles caused by bundling, and manufacturing workmanship of parts. Cognitive uncertainty factors mainly refer to interval estimates due to lack of knowledge, e.g., cognitive uncertainty in physical parameters and uncertainty due to simplified simulation models. Uncertainty analysis refers to the quantitative prediction of the effect of input randomness on output results. This usually includes expectation values, standard deviation values, worst-case estimates, and probability density curves. The application of uncertainty analysis methods can enhance the credibility of electromagnetic prediction results, thereby significantly improving the reliability and practicality of electromagnetic protection design.

The uncertainty factor is described using a random variable model in vector form as follows.

$$\xi = \{\xi_1, \xi_2, \dots, \xi_j, \dots, \xi_M\} \quad (3)$$

where  $\xi_j$  is the random variable,  $\xi$  the vector of random variables, and  $M$  the number of random variables.

Based on the weak large number law, the random variable vector  $\xi$  can be described using exhaustive sampling points  $S_1 = [\psi_1, \psi_2, \dots, \psi_{n2}]$ , that is, considering all possible cases, where the number of sampling points is  $n2$ , and  $n2 \gg n1$ . Each sampling point  $\psi_i$  is  $M$ -dimensional vector data as follows.

$$\psi_i = \{\psi_i(1), \psi_i(2), \dots, \psi_i(j), \dots, \psi_i(M)\} \quad (4)$$

where  $\psi_i(j)$  is a definite constant value. It is worth noting that  $\xi_j$  in Equation (3) corresponds to  $\psi_i(j)$  in Equation (4) as shown in Figure 1.

Each random variable  $\xi_j$  in the uncertainty analysis is sampled according to its probability density function (PDF), and their PDF can be different as shown in Equation (5). For example, in the vector  $\xi$  of random variables, it may be the case that  $\xi_1$  follows a uniform distribution;  $\xi_2$  follows a normal distribution; and  $\xi_3$  follows a Gaussian distribution.

$$\xi_j \sim \text{PDF}_j(\xi_j) \quad (5)$$

When the surrogate model is applied to uncertainty analysis, firstly representative sampling points in the exhaustive sampling space  $S_1$  are selected by a certain sampling method. Here, the representative sampling points are the sample space  $S_{EMC}$  of the training set  $(S_{EMC}, Y_{EMC})$ . Then, the surrogate model  $M_{Kriging}[\cdot]$  is trained based on the training set  $(S_{EMC}, Y_{EMC})$ . The sampling points  $\psi_i$  in the exhaustive sampling space  $S_1$  are brought into the surrogate model one by one, as shown in Equation (6). The EMC simulation results  $Y_{Kriging}$  based on the Kriging model are obtained and then statistically analyzed to obtain the uncertainty analysis results such as expectation, standard deviation, worst-case estimates, and probability density curves.

$$Y_{Kriging} = M_{Kriging}[\psi_i] \quad (6)$$

## 2.2. Electromagnetic Optimization Design

In electromagnetic optimization design, the parameters to be optimized are also varied in a certain range. It is assumed that there are  $n3$  ( $n3 \gg n1$ ) parameters  $\omega_i$  to be optimized, which are varied in the range of  $[a_i, b_i]$ . In EMC simulation, each parameter  $\omega_i$  will have an impact on the simulation results, so the raster point space  $S_2$  shown in Equation (7) is obtained.

$$S_2 = \omega_1 \otimes \omega_2 \otimes \dots \otimes \omega_i \otimes \dots \otimes \omega_{n3} \quad (7)$$

When surrogate models are applied to electromagnetic optimization design,  $S_{EMC}$  is first selected in the raster point space  $S_2$  by a certain sampling method. Then, the surrogate model  $M_{Kriging}[\cdot]$  is trained based on the training set  $(S_{EMC}, Y_{EMC})$ . The raster points in the raster point space  $S_2$  are brought into the surrogate model  $M_{Kriging}[\cdot]$ . The obtained simulation results are optimized to find the optimal solution for EMC simulation. In this paper, the maximum crosstalk voltage of the cascaded cable model is taken as the optimal solution.

## 3. STATIC SAMPLING STRATEGY AND SEQUENTIAL ADDITION STRATEGY

When the surrogate model is applied to uncertainty analysis and electromagnetic optimization design in EMC simulation, the sampling strategy used to obtain the sample space  $S_{EMC}$  is the key to determining the accuracy of the surrogate model.

In this paper, two sampling strategies are applied to obtain the sampling space  $S_{EMC}$ . The first sampling strategy is the static sampling strategy, that is, obtaining all the sampling points in  $S_{EMC}$  at once. This sampling strategy has a high degree of coverage. The sampling points are all distributed as uniformly as possible to cover all parts of the parameter space. The static sampling strategy is most commonly used in EMC simulations based on surrogate models.

The second sampling strategy is the sequential addition strategy, as shown in Figure 2. Its initial sampling space  $S_0$  has only a rather small number of sampling points  $x_0(k)$ , and deterministic EMC simulations are performed on  $x_0(k)$  to obtain the simulation result  $y_0(k)$ . The surrogate model is constructed based on the obtained data pairs  $\{x_0(k), y_0(k)\}$ . The optimal result and its corresponding sampling point  $x_i$  are found by the Genetic Algorithm (GA). If the number of sampling points does

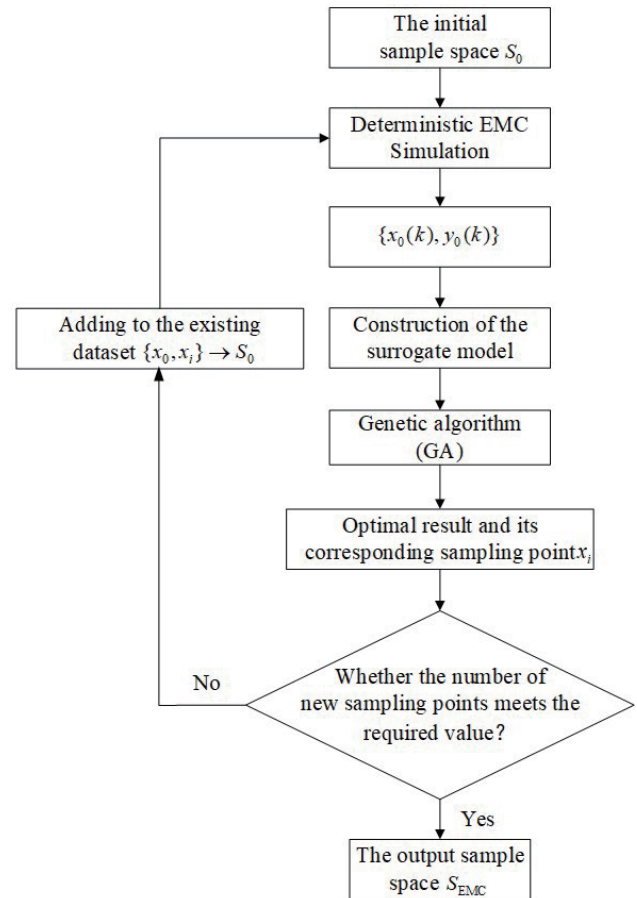


FIGURE 2. Flowchart of the sequential addition strategy.

not reach the required value, the new sampling point is added to the existing sampling space  $S_0$  to build a new surrogate model. If the number of sampling points reaches the required value, all the sampling points in  $S_{EMC}$  obtained by the sequential addition strategy are output. It is noted that the sampling space  $S_{EMC}$  obtained by the two sampling strategies is different.

To clearly discuss the two sampling strategies, this section develops mathematical models for uncertainty analysis and optimization design. These models will be applied in the EMC simulation examples presented in the next section. The uncertainty analysis model is a mathematical model containing two random variables  $\{\xi_1, \xi_2\}$  with independent variables  $X_1$  and  $X_2$  (The  $x$ -axis coordinates of the two red transmission lines in Figure 6). The results of applying random variable modeling are shown below.

$$\begin{cases} X_1(\xi_1) = 1.5 + 0.5 \times \xi_1 \\ X_2(\xi_2) = 1.5 + 0.5 \times \xi_2 \end{cases} \quad (8)$$

where  $X_1$  and  $X_2$  are uniformly distributed random variables in the interval  $[-1, 1]$ .

The optimization design model is also a mathematical model with independent variables  $X_1$  and  $X_2$ . The range of values is shown in equation (9).

$$\begin{aligned} 1 &\leq X_1 \leq 2 \\ 1 &\leq X_2 \leq 2 \end{aligned} \quad (9)$$

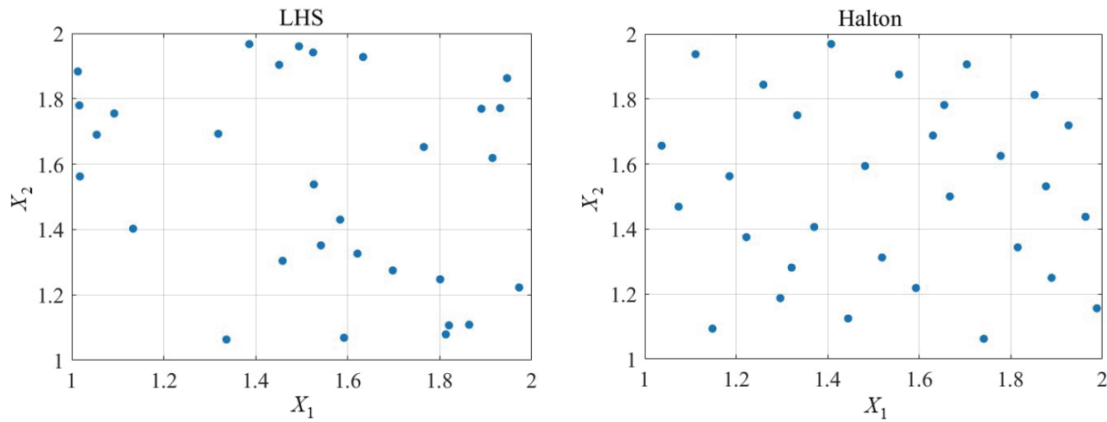


**FIGURE 3.** The schematic diagram of sampling points for LHS and Halton selection based on the static sampling strategy.

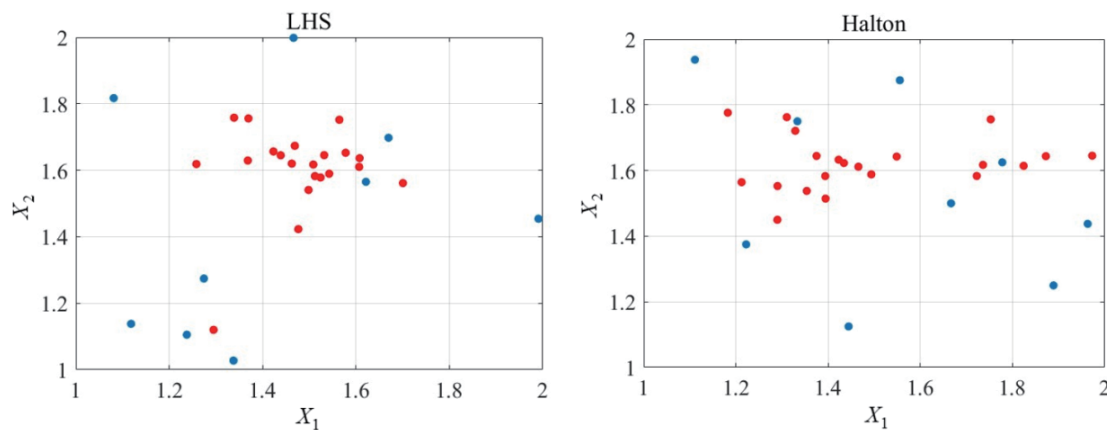


**FIGURE 4.** The schematic diagram of sampling points for LHS and Halton selection based on the sequential addition strategy.

The independent variables  $X_1$  and  $X_2$  of both mathematical models take values in the range  $[1, 2]$ .

In this paper, two sampling methods, Latin Hypercube Sampling (LHS) [8] and Halton Sampling (Halton) [9], are applied to two sampling strategies. LHS is a stratified sampling method that evenly divides the range of each dimension into  $n$  intervals and then randomly selects a point within each interval. Halton is a low-discrepancy sequence, and these sequences utilize prime bases to produce a set of sample points with low variability. The number of sampling points for a given sampling space  $S_{\text{EMC}}$  is 30. The schematic diagram of the sampling points selected by LHS and Halton based on the static sampling strategy is shown in Figure 3, where 30 sampling points are selected at one time. The schematic diagram of the sampling points for LHS and Halton selection based on the sequential addition strategy is shown in Figure 4. Firstly, 9 sampling points of the initial sampling space  $S_0$  are selected by LHS and Halton (blue points in the figure). Then, the number of sampling points is expanded to 30, that is, 21 additional sampling points are added through the sequential addition strategy (red points in the figure). The sampling points in Figure 3 and Figure 4 are applied in the EMC example in the next section.

The flowchart of constructing the surrogate model based on two sampling strategies and applying it to two scenarios

of uncertainty analysis and electromagnetic optimization design is shown in Figure 5. Firstly, the LHS and Halton based on the sequential addition strategy and static sampling strategy are applied to the sample to obtain four sampling spaces of  $S_{\text{EMC}1}$ ,  $S_{\text{EMC}2}$ ,  $S_{\text{EMC}3}$ , and  $S_{\text{EMC}4}$ , as shown in the scatter plots in Figures 3 and 4. Four training sets,  $\{S_{\text{EMC}1}, Y_{\text{EMC}1}\}$ ,  $\{S_{\text{EMC}2}, Y_{\text{EMC}2}\}$ ,  $\{S_{\text{EMC}3}, Y_{\text{EMC}3}\}$ , and  $\{S_{\text{EMC}4}, Y_{\text{EMC}4}\}$ , are obtained through deterministic EMC simulation, which in turn leads to the construction of four Kriging surrogate models,  $M_{\text{Kriging}}^1[\cdot]$ ,  $M_{\text{Kriging}}^2[\cdot]$ ,  $M_{\text{Kriging}}^3[\cdot]$ , and  $M_{\text{Kriging}}^4[\cdot]$ . Finally, uncertainty analysis and electromagnetic optimization design are performed. The results of the uncertainty analysis and electromagnetic optimization design are used to determine the applicability of different sampling strategies.

#### 4. CROSSTALK EXAMPLE FOR CASCADING CABLE MODEL

In this paper, the cascaded cable crosstalk example is applied to explore the applicability of two sampling strategies in uncertainty analysis and electromagnetic optimization design. In order to describe the geometric randomness induced by bundling or other factors, cascaded transmission line models are commonly used to model cables [10]. Figure 6 shows a schematic diagram of a cascaded cable model with two cables lying flat

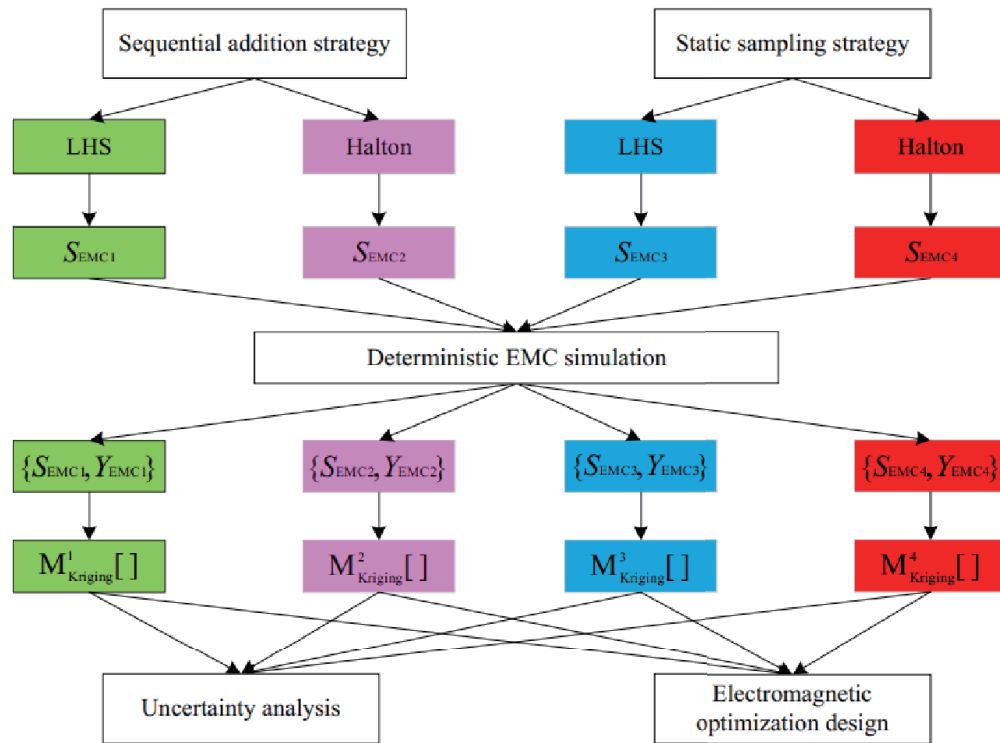


FIGURE 5. Flowchart of uncertainty analysis and electromagnetic optimization design based on two sampling strategies.

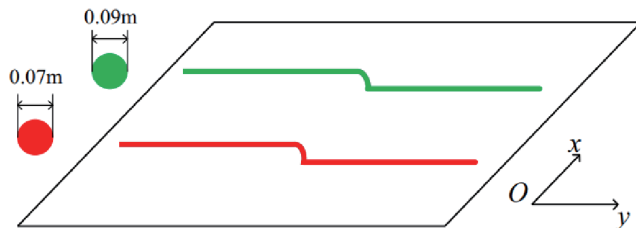


FIGURE 6. Schematic diagram of cascaded cable model.

on a ground aluminum plate, each of which consists of two uniform transmission lines cascaded together. The red line is the interference transmitting line with a diameter of 0.07 meters. The green line is the interference receiving line with a diameter of 0.09 meters. In this example, the geometric position of the cable can be changed only in the  $x$ -axis direction.

Figure 7 shows the schematic diagram of the circuit for the crosstalk problem. The length of both the interference transmitting line and interference receiving line is 1 m. Each end of the interference receiving line is connected to a  $50\ \Omega$  load, and the interference transmitting line needs to be connected not only to the  $50\ \Omega$  load but also to the sinusoidal excitation source  $U_m$ . The amplitude of  $U_m$  is 1 V. The strength of the crosstalk between the cables is characterized by the voltage value  $V_{far}$  at the far end of the interference receiving line. The heights between these two cables and the ground are their radii, that is 0.045 m and 0.035 m. Assuming that the  $x$ -axis coordinates of the two transmission lines of the interference transmitting line are fixed, they are 1.3 m and 1.6 m. The  $x$ -axis coordinates of

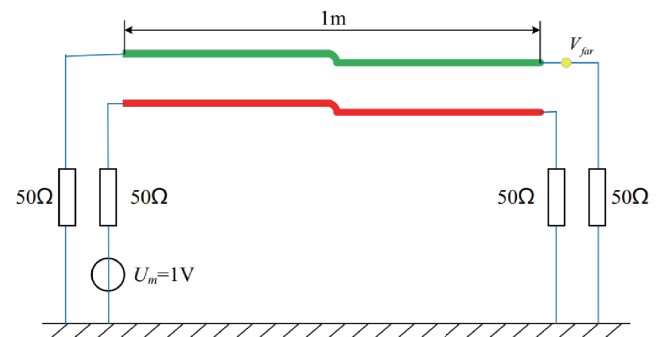
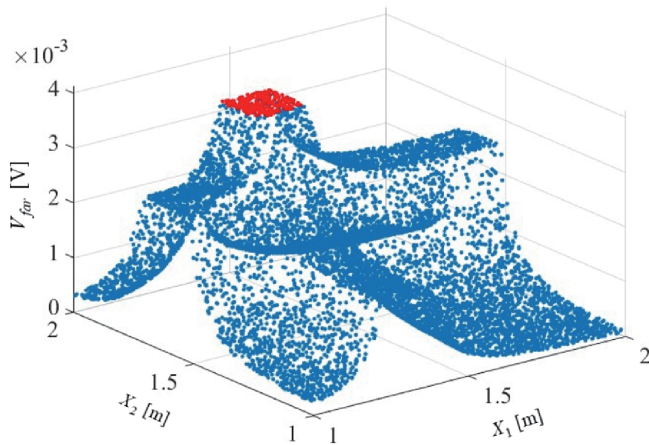


FIGURE 7. Schematic diagram of cascaded cable model crosstalk example.

the two transmission lines of the interference receiving line,  $X_1$  and  $X_2$ , are varied within the range of [1 m, 2 m], which is the mathematical model established by formula (8) and formula (9) in the last section. The sampling points for the two sampling strategies are shown in Figure 3 and Figure 4. More introduction to cable crosstalk example can be found in [11]. In this paper, the mirror method and electrical axis method are applied to give the electrical parameters in the transmission line model. The Finite Difference Time Domain (FDTD) method is applied to calculate the crosstalk voltage  $V_{far}$  at the far end of the interference receiving line. FDTD can be found specifically in the research of Sun et al. [12].

According to electromagnetic field theory, closer proximity between cables increases the strength of electromagnetic coupling and enhances crosstalk between the lines. According





**FIGURE 8.** The scatter plots of MCM result for cascaded cable model crosstalk at 2 MHz.

to this theorem, an electromagnetic optimization design problem with known optimization results can be constructed by the cascade model. The crosstalk value is maximized when the two cables overlap, so the answer for the optimal design is  $X_1 = 1.3$  m,  $X_2 = 1.6$  m. At this point, the crosstalk voltage is 0.0041 V for a frequency of 2 MHz and 0.0079 V for 40 MHz. It is worth noting that since the cables in the example are solid (have a radius), they cannot overlap exactly. Therefore, the distance  $d$  between the interference transmitting line and interference receiving line is directly equal to 0.08 m when  $d$  is less than the sum of the radii of the two cables  $0.045 + 0.035 = 0.08$  m.

## 5. APPLICATION OF TWO SAMPLING STRATEGIES TO UNCERTAINTY ANALYSIS AND ELECTROMAGNETIC OPTIMIZATION DESIGN

In this section, the cascade cable example proposed in the last section is applied to verify the applicability of the sequential addition strategy and static sampling strategy in uncertainty analysis and electromagnetic optimization design. The simulation results at 2 MHz and 40 MHz are analyzed to determine which sampling strategy is more accurate for constructing the surrogate model in two EMC simulation scenarios, which are uncertainty analysis and electromagnetic optimization design.

The Monte Carlo Method (MCM) can be used in uncertainty analysis and electromagnetic optimization design [11, 13] and is generally considered to be one of the most reliable methods due to its high accuracy. However, the computational efficiency of MCM is extremely low and cannot be effectively applied to complex EMC problems. It is often used as a reference method in uncertainty analysis to validate other uncertainty analysis methods [14]. MCM performs deterministic EMC simulations on exhaustive sampling points. To ensure convergence, MCM uses 10000 sampling points. Scatter plots of cable crosstalk voltages are obtained, Figure 8 for 2 MHz and Figure 9 for 40 MHz. The scatter plots show the crosstalk voltage  $V_{far}$  of the MCM at 10,000 samples. Since the cable radius is solid, the distance  $d$  between the interference transmitting line and interference receiving line is equal to 0.08 m when

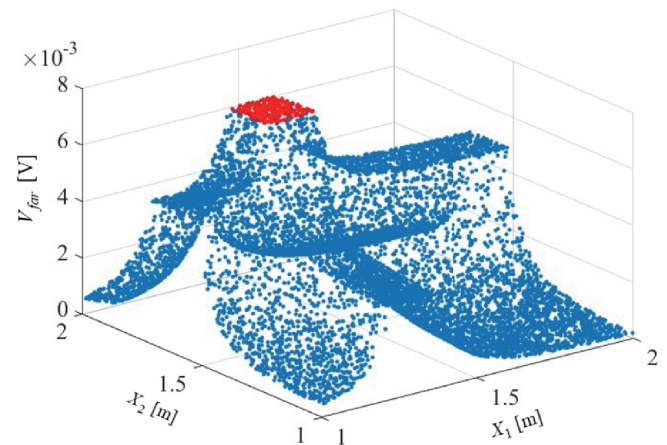


**FIGURE 9.** The scatter plots of MCM result for cascaded cable model crosstalk at 40 MHz.

$1.22 \text{ m} \leq X_1 \leq 1.38 \text{ m}$  and  $1.52 \text{ m} \leq X_2 \leq 1.68 \text{ m}$ . The red points in the figure are the maximum values of the crosstalk value  $V_{far}$ . The maximum crosstalk voltage is 0.0041 V at 2 MHz and 0.0079 V at 40 MHz.

The LHS and Halton based on the sequential addition strategy are denoted as SAS-LHS and SAS-Halton, respectively. The LHS and Halton based on the static sampling strategy are denoted as SSS-LHS and SSS-Halton, respectively.

When the uncertainty analysis is performed, the simulation results of Kriging based on four sampling methods are examined using the MCM simulation results as the standard. In this paper, the Mean Equivalent Area Method (MEAM) is applied to quantitatively evaluate the difference between uncertainty simulation data and standard data [15]. The evaluation result is a constant between 0 and 1. The closer the value is to 1, the smaller the difference and the more accurate the uncertainty analysis method is. Figure 10 shows the results of the uncertainty analysis of the crosstalk voltage values at the far end of the interference receiving line at 2 MHz, expressed in the form of probability density. Figure 11 shows the probability density curve at 40 MHz. The probability density curves of the two plots demonstrate the same conclusion that the Kriging model based on the static sampling strategy is similar to the MCM results. It can be tentatively concluded that the uncertainty analysis results of SSS-LHS and SSS-Halton are more accurate. Table 1 shows the evaluation results of MEAM. Based on the MEAM results at two frequency points (2 MHz and 40 MHz), it is evident that the Kriging model, constructed using SSS-LHS and SSS-Halton, demonstrates higher accuracy and closely matches the MCM simulation results in the uncertainty analysis. So the static sampling strategy is more suitable for uncertainty analysis, because of its good coverage and uniformity in the sampling process.

When the electromagnetic optimization design is carried out, the Kriging model is constructed based on four sampling methods, namely, SSS-Halton, SAS-Halton, SSS-LHS, and SAS-LHS, and the optimal solution is obtained through optimization search to obtain the maximum value of crosstalk voltage. Table 2 shows the optimization results at 2 MHz, and Table 3

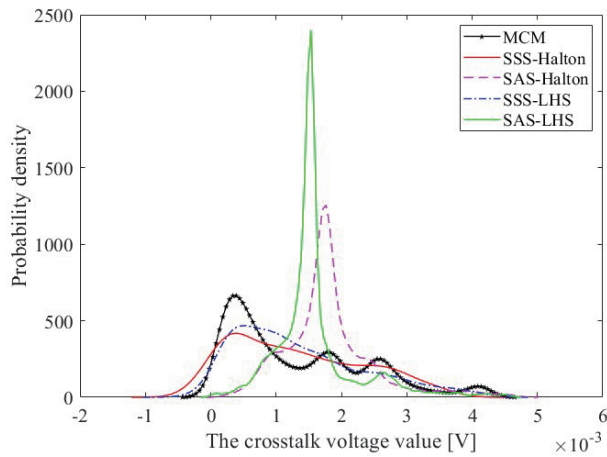


**FIGURE 10.** The probability density of crosstalk voltage values at 2 MHz.

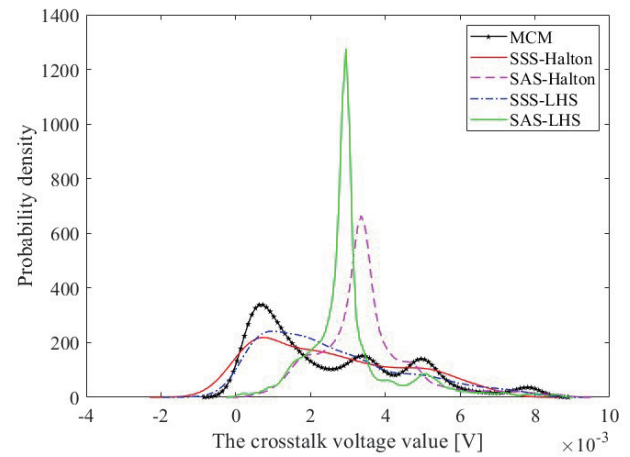


**FIGURE 11.** The probability density of crosstalk voltage values at 40 MHz.

**TABLE 1.** The results of the MEAM evaluation.

	The MEAM value of 2 MHz	The MEAM value of 40 MHz
<b>SSS-Halton</b>	0.9479	0.9506
<b>SAS-Halton</b>	0.6557	0.6539
<b>SSS-LHS</b>	0.9306	0.9327
<b>SAS-LHS</b>	0.6079	0.6075

**TABLE 2.** The optimization results of 2 MHz.

	The optimization result	The crosstalk voltage value
<b>SSS-Halton</b>	$\{X_1 = 1.2323 \text{ m}, X_2 = 1.7013 \text{ m}\}$	0.0037 V
<b>SAS-Halton</b>	$\{X_1 = 1.2903 \text{ m}, X_2 = 1.5528 \text{ m}\}$	0.0041 V
<b>SSS-LHS</b>	$\{X_1 = 1.3821 \text{ m}, X_2 = 1.6410 \text{ m}\}$	0.0040 V
<b>SAS-LHS</b>	$\{X_1 = 1.2582 \text{ m}, X_2 = 1.6187 \text{ m}\}$	0.0041 V

**TABLE 3.** The optimization results of 40 MHz.

	The optimization result	The crosstalk voltage value
<b>SSS-Halton</b>	$\{X_1 = 1.2008 \text{ m}, X_2 = 1.6154 \text{ m}\}$	0.0070 V
<b>SAS-Halton</b>	$\{X_1 = 1.3749 \text{ m}, X_2 = 1.6443 \text{ m}\}$	0.0079 V
<b>SSS-LHS</b>	$\{X_1 = 1.3846 \text{ m}, X_2 = 1.5093 \text{ m}\}$	0.0068 V
<b>SAS-LHS</b>	$\{X_1 = 1.3683 \text{ m}, X_2 = 1.6294 \text{ m}\}$	0.0079 V

shows the optimal solution at 40 MHz. When the frequency is 2 MHz, the crosstalk voltage obtained by the optimization based on SAS-Halton and SAS-LHS is 0.0041 V, while the crosstalk voltage obtained by the optimization based on SSS-Halton and SSS-LHS is 0.0037 V and 0.0040 V, respectively. When the frequency is 40 MHz, the optimization results based on SAS-Halton and SAS-LHS are 0.0079 V, while the optimization results based on SSS-Halton and SSS-LHS are 0.0070 V and 0.0068 V, respectively. It can be seen that although the op-

timization results based on the Kriging model constructed by the four sampling methods are all relatively good, obviously, the sequential addition strategy is more suitable for electromagnetic optimization design.

## 6. DISCUSSION ON FUTURE RESEARCH WORK

In two EMC simulation scenarios, uncertainty analysis and electromagnetic optimization design, the surrogate model sam-

ple points convergence determination is the next step of the research conducted. If the convergence of the surrogate model in different application scenarios can be predicted, it will help to improve the computational efficiency and the credibility of the simulation results.

## 7. CONCLUSION

In this paper, two sampling strategies, the sequential addition strategy and the static sampling strategy, are applied to the construction of the EMC surrogate model to investigate which sampling strategy is applied to construct the surrogate model with higher accuracy in two EMC simulation scenarios, which are uncertainty analysis and electromagnetic optimization design. The surrogate models constructed based on the two sampling strategies are applied to the cascade cable crosstalk example for uncertainty analysis and electromagnetic optimization design, respectively. Based on the simulation results, it is concluded that the surrogate model constructed using the sequential addition strategy is more suitable for electromagnetic optimization design, whereas the model constructed with the static sampling strategy is more appropriate for uncertainty analysis. This research provides theoretical-level suggestions for applying surrogate models in EMC simulations, enhancing their effectiveness in uncertainty analysis and electromagnetic optimization design.

## ACKNOWLEDGEMENT

This work is supported in part by the Youth Science Foundation Project, National Natural Science Foundation of China, under Grant 52301414.

## REFERENCES

- [1] Trinchero, R., M. Larbi, H. M. Torun, F. G. Canavero, and M. Swaminathan, "Machine learning and uncertainty quantification for surrogate models of integrated devices with a large number of parameters," *IEEE Access*, Vol. 7, 4056–4066, 2018.
- [2] Ren, Z., J. Ma, Y. Qi, D. Zhang, and C.-S. Koh, "Managing uncertainties of permanent magnet synchronous machine by adaptive Kriging assisted weight index Monte Carlo simulation method," *IEEE Transactions on Energy Conversion*, Vol. 35, No. 4, 2162–2169, Dec. 2020.
- [3] Hu, B., Y. Wang, S. Huo, and J. Bai, "Application of improved SROM based on RBF neural network model in EMC worst case estimation," *Progress In Electromagnetics Research Letters*, Vol. 119, 51–57, 2024.
- [4] Biondi, A., D. V. Ginste, D. D. Zutter, P. Manfredi, and F. G. Canavero, "Variability analysis of interconnects terminated by general nonlinear loads," *IEEE Transactions on Components, Packaging and Manufacturing Technology*, Vol. 3, No. 7, 1244–1251, Jul. 2013.
- [5] Shen, J., H. Yang, and J. Chen, "Analysis of electrical property variations for composite medium using a stochastic collocation method," *IEEE Transactions on Electromagnetic Compatibility*, Vol. 54, No. 2, 272–279, Apr. 2012.
- [6] Li, H., B. Zhu, and J. Chen, "Optimal design of photonic band-gap structure based on kriging surrogate model," *Progress In Electromagnetics Research M*, Vol. 52, 1–8, 2016.
- [7] Bai, J., B. Hu, and Z. Xue, "EMC uncertainty simulation method based on improved kriging model," *IEEE Letters on Electromagnetic Compatibility Practice and Applications*, Vol. 5, No. 4, 127–130, Dec. 2023.
- [8] Davey, K. R., "Latin hypercube sampling and pattern search in magnetic field optimization problems," *IEEE Transactions on Magnetics*, Vol. 44, No. 6, 974–977, Jun. 2008.
- [9] Lin, Z., G. Xie, W. Xu, J. Han, and Y. Zhang, "Accelerating stochastic computing using deterministic halton sequences," *IEEE Transactions on Circuits and Systems II: Express Briefs*, Vol. 68, No. 10, 3351–3355, Oct. 2021.
- [10] Beerten, J., S. D'Arco, and J. A. Suul, "Frequency-dependent cable modelling for small-signal stability analysis of VSC-HVDC systems," *IET Generation, Transmission & Distribution*, Vol. 10, No. 6, 1370–1381, Apr. 2016.
- [11] Bai, J., G. Zhang, D. Wang, A. P. Duffy, and L. Wang, "Performance comparison of the SGM and the SCM in EMC simulation," *IEEE Transactions on Electromagnetic Compatibility*, Vol. 58, No. 6, 1739–1746, Dec. 2016.
- [12] Sun, Y., J. Liu, Z. Su, X. Wang, and F. Liang, "Analysis of FDTD crosstalk of multiconductor overhead transmission lines with a frequency-varying ground impedance loss," in *2020 IEEE International Symposium on Electromagnetic Compatibility & Signal/Power Integrity (EMCSI)*, 29–33, Reno, NV, USA, Jul. 2020.
- [13] Lagouanelle, P., F. Freschi, and L. Pichon, "Adaptive sampling for fast and accurate metamodel-based sensitivity analysis of complex electromagnetic problems," *IEEE Transactions on Electromagnetic Compatibility*, Vol. 65, No. 6, 1820–1828, Dec. 2023.
- [14] Bai, J., B. Hu, S. Huo, and M. Li, "Uncertainty analysis method for electromagnetic compatibility simulation based on random variable black box model," *Progress In Electromagnetics Research M*, Vol. 123, 23–33, 2024.
- [15] Bai, J., J. Sun, and N. Wang, "Convergence determination of EMC uncertainty simulation based on the improved mean equivalent area method," *The Applied Computational Electromagnetics Society Journal (ACES)*, Vol. 36, No. 11, 1446–1452, Dec. 2021.